LETTERS

Controlled multiple reversals of a ratchet effect

Clécio C. de Souza Silva[1]†, Joris Van de Vondel[1], Mathieu Morelle[1] & Victor V. Moshchalkov[1]

A single particle confined in an asymmetric potential demonstrates an anticipated ratchet effect by drifting along the 'easy' ratchet direction when subjected to non-equilibrium fluctuations[1–3]. This well-known effect can, however, be dramatically changed if the potential captures several interacting particles. Here we demonstrate that the inter-particle interactions in a chain of repelling particles captured by a ratchet potential can, in a controllable way, lead to multiple drift reversals, with the drift sign alternating from positive to negative as the number of particles per ratchet period changes from odd to even. To demonstrate experimentally the validity of this very general prediction, we performed transport measurements on a.c.-driven vortices trapped in a superconductor by an array of nanometre-scale asymmetric traps. We found that the direction of the vortex drift does undergo multiple reversals as the vortex density is increased, in excellent agreement with the model predictions. This drastic change in the drift behaviour between single- and multi-particle systems can shed some light on the different behaviour of ratchets and biomembranes[4] in two drift regimes: diluted (single particles) and concentrated (interacting particles).

Contrary to what intuition could perhaps tell us, particles in a ratchet potential can, under special conditions, move preferentially along the direction where the potential barriers are steeper, that is, along the 'hard' direction. This effect can be crucial in the design of artificial ratchet-based devices capable of shuttling or separating—for instance, colloidal suspensions[5] and DNA molecules[6]. In theory, an inversion in the drift direction of a single-particle brownian ratchet is predicted to occur for non-zero thermal noise when the excitation frequency exceeds a certain critical value, which is usually high and very sensitive to the model parameters[7]. In a system of many weakly interacting particles, this effect can, however, be strongly reduced when the particle density is increased[8]. Drift inversions have also been observed in mixtures of interacting brownian particles[9] and in chaotic underdamped ratchets at zero thermal noise[10]. Here we show that, in a system of strongly interacting particles in a ratchet potential, the drift direction undergoes controllable multiple sign inversions as a function of particle density. These inversions do not require thermal or chaotic noise, or high excitation frequencies or a mixture of particles. Rather, they are ruled deterministically by the internal degrees of freedom of the system, providing a simple way to tune the drift direction of ratchet devices.

We consider a one-dimensional (1D) system of particles interacting via the pair potential $V_{\rm int}(r) = -E_0 \ln(r)$, with r the pair separation and E_0 the relevant energy scale, in the double-well ratchet potential

$$U_{\rm p}(x) = -U_{\rm p1} e^{-\sin^2(\pi x)/2\sin^2(\pi R)} - U_{\rm p2} e^{-\sin^2(\pi(x-d))/2\sin^2(\pi R)} \qquad (1)$$

where $U_{\rm p1}$ and $U_{\rm p2}$ determine the depth of the stronger and weaker wells, respectively, which are separated by a distance $d = 0.36$ and have width $R = 0.15$, and x is the position. All lengths are in units of the ratchet period a. The dynamics of the chain is studied by molecular dynamics simulations of the Langevin equations,

$$m\ddot{x}_i = -\eta\dot{x}_i - \sum_j \nabla V_{\rm int}(x_i - x_j) - \nabla U_{\rm p}(x) + F + \Gamma_i \qquad (2)$$

where m is the mass of the particles, η the friction coefficient, F the external drive, and Γ_i the gaussian thermal noise[11]. Hereafter we adopt $m = 1$ and $\eta = 16$, which corresponds to strongly overdamped dynamics.

Figure 1a shows density plots of the effective asymmetry in the critical forces for drifting the particles to the positive (F_{c+}) and to the negative (F_{c-}) direction, $\alpha_{\rm eff} = 1 - F_{c+}/F_{c-}$. The sign of $\alpha_{\rm eff}$ determines the preferential drift direction—positive ('easy') direction for $\alpha_{\rm eff} > 0$ and negative ('hard') direction for $\alpha_{\rm eff} < 0$—whereas its magnitude is a measure of the ratchet efficiency. The plots are presented in the $\tilde{U}_{\rm p1}$–β plane ($\tilde{U}_{\rm p1} = U_{\rm p1}/E_0$ determines the potential strength relative to inter-particle interactions and $\beta = U_{\rm p1}/U_{\rm p2}$ determines the potential asymmetry) for occupation number $n = 1$, 2, 3 and 4 particles per ratchet period and for zero noise ($T = 0$). For $n = 1$ the particles are more easily driven to the usual positive direction ($\alpha_{\rm eff} > 0$) and, except for $\tilde{U}_{\rm p1} < 1$ (where the potential cannot trap the chain effectively), $\alpha_{\rm eff}$ varies only with β. However, for $n > 1$, $\alpha_{\rm eff}$ has a much richer dependence on the ratchet potential parameters, assuming either positive or negative values with comparable intensity. Particularly, there is a large region of the phase diagrams ($\beta > 0.56$ and moderate pinning strengths) where $\alpha_{\rm eff}$ is always positive for odd n and negative for even n. In this region, particles distribute evenly between the weak and strong pinning sites for even n, whereas for odd n the strong traps capture one particle more than the weak ones (Fig. 1b).

A simple way to understand this interesting effect is to consider each local well in a ratchet period as being characterized by the effective energies E_1 ('strong' well) and E_2 ('weak' well). For $n = 0$, the strong trap yields a lower energy than the weak one ($E_1(0) < E_2(0)$). For $n = 1$, the particle occupies the strong well, raising its effective energy enough to surpass the energy of the (empty) trap 2 ($E_1(1) > E_2(0)$). A second particle will find a stable position at trap 2, then raising its energy above $E_1(E_1(1) < E_2(1))$. By increasing n even further, the rise in the effective energies proceeds following a brick-wall tiling pattern, with the particles populating each trap alternately. Thus, for n even, there is necessarily a smaller energy input required to move one particle from trap 2 (across the small inner energy barrier) to trap 1 (as $E_1(n_1) < E_2(n_2 = n_1)$), whereas for odd n a transition from 1 to 2 is favoured (as $E_1(n_1) > E_2(n_2 = n_1 - 1)$). Particles that are the closest to the inner energy barrier are the natural candidates to undergo such transitions. In this sense, these particles are the most weakly pinned ones.

As a first demonstration of the ratchet mechanism in this system, we excite the particles with an a.c. square-wave drive with an amplitude just above the threshold force (defined as $F_{\rm thresh} = \min(F_{c+}, F_{c-})$) of the corresponding chain and a very low frequency (adiabatic drive). As illustrated in Fig. 1c, the motion of the weakly

[1]INPAC—Institute for Nanoscale Physics and Chemistry, Nanoscale Superconductivity and Magnetism Group, Katholieke Universiteit Leuven, Celestijnenlaan 200 D, B-3001 Leuven, Belgium. †Present address: Departamento de Física, Universidade Federal de Pernambuco, 50670-901 Recife-PE, Brazil.

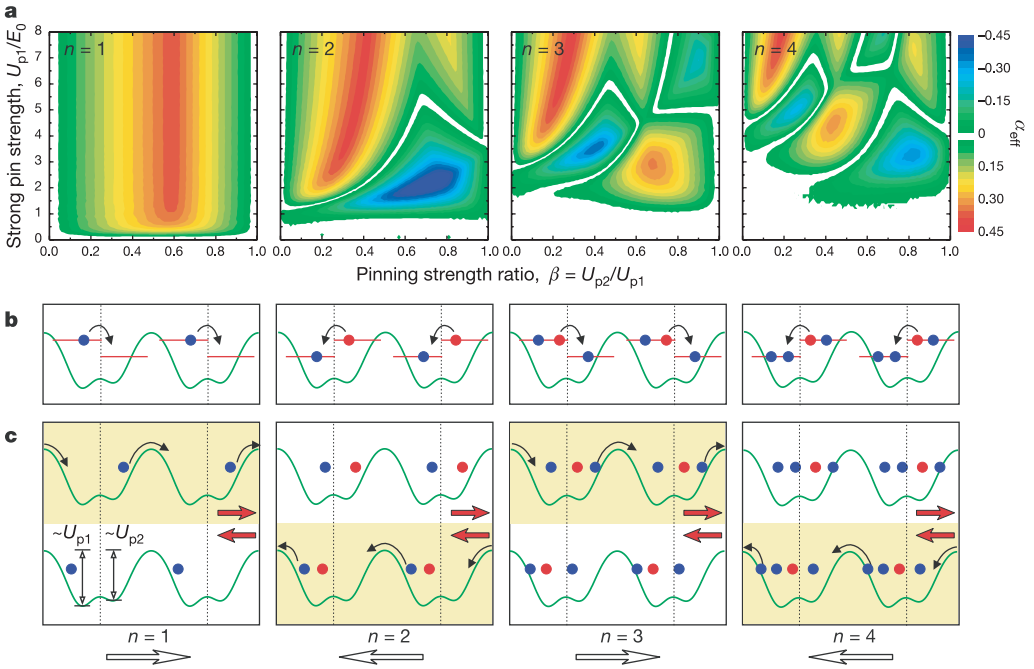

Figure 1 | Effective asymmetry and schematic demonstration of the ratchet mechanism. a, Density plots of the effective asymmetry $\alpha_{eff} = 1 - F_{c+}/F_{c-}$ as a function of the ratchet parameters $\tilde{U}_{p1} = U_{p1}/E_0$ and $\beta = U_{p2}/U_{p1}$ (<1) for $n = 1$ to 4 (see text for details). The potential has one minimum per period for $\beta < 0.56$ and two local minima per period for $\beta > 0.56$. We forced white shading for $\alpha_{eff} = 0$ to enhance the contrast between the positive and negative drift phases. The critical forces F_{c+} and F_{c-} were obtained by varying the driving force quasi-statically to the positive and negative directions respectively and assuming as a criterion for macroscopic drift that all particles travel a distance of at least one ratchet period. **b**, Diagram of the equilibrium configurations for $n = 1$ to 4 obtained by annealing the chain down to zero temperature with $U_{p1}/E_0 = 3.2$ and $U_{p2} = 0.9U_{p1}$, which generates a double-well ratchet potential (green curves). The relative characteristic energies of each pinning well (the energy of a well plus the energy of the trapped vortices) and their respective occupancies are schematically represented. Owing to the excess in energy, one particle in a higher-energy trap is 'looser' than the others. Such particle (marked in red) is the most favourable for performing a transition (black arrows) through the inner energy barrier. **c**, Schematic demonstration of the ratchet mechanism when the chain is excited by an a.c. square-wave force with an amplitude just above the threshold force. Red arrows indicate the force direction. Yellow backgrounds highlight macroscopic motion of the chain in the corresponding drive direction, whereas white backgrounds indicate that the chain is at rest (pinned). The macroscopic drift is triggered by a transition of the most weakly pinned particle to the next available pinning site, as indicated in **b**. In sequence, one particle in this site is knocked out to the next ratchet period (as indicated by the black arrows), starting up motion of the whole chain.

pinned particle across the inner energy barrier triggers the whole ratchet mechanism (see also the Supplementary Videos). After transition, this particle 'overpopulates' the target well, which then releases another particle to the next ratchet period. When the drive inverts its sign, no motion is detected. This produces a net rectified motion with positive direction for odd n and negative direction for even n. To study in more detail the dependence of rectification on n, we calculated the net velocity of the chain as a function of n and $\tilde{U}_{p1}$ for a constant sinusoidal a.c. bias (Fig. 2). The result demonstrates remarkable sign reversals every time n approaches an integer value. We have also tested these predictions for the well-known double-sine potential[7] (sketches of this and the double-well potentials are provided in Supplementary Fig. S1). In a large range of the potential parameters multiple reversals were also observed (compare Supplementary Fig. S2). To evaluate further the generality of our findings, we performed similar calculations for other friction values

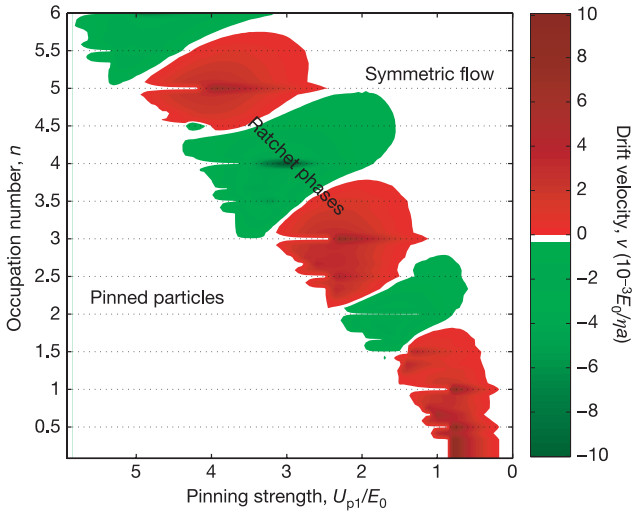

Figure 2 | Net drift velocity of the chain as a function of occupation number and pinning strength. The chain was adiabatically excited with a sinusoidal forcing of amplitude $F_{ac} = 3E_0/a$ and frequency $f = 5 \times 10^{-7}\ m/\eta$ at zero thermal noise (here a is the ratchet period, m is the particle mass, and η is the friction coefficient). The simulation cell comprises 12 periods of the double-well ratchet potential ($U_{p1}/E_0 = 3.2$ and $U_{p2} = 0.9U_{p1}$) with periodic boundary conditions. The U_{p1}/E_0 axis is presented in decreasing order for further comparison with Fig. 3c. The white areas may correspond to a pinned phase, where particles just oscillate inside the traps, or a symmetric moving phase. Also indicated are the ratchet phases exhibiting multiple sign inversions. The chain is rectified with maximum efficiency at integer and half-integer occupation numbers.

down to $\eta = 2$, which corresponds to the (regular) underdamped regime. In general, the results are very similar to those presented in Figs 1 and 2.

To test these predictions experimentally, we performed transport measurements of a.c.-driven vortices in a nanostructured superconducting film with an array of asymmetrical pinning sites. Vortices are whirlpools of current carrying one quantum of magnetic flux ($\Phi_0 = 2.07 \times 10^{-15}$ Wb) that repel each other and are attracted by microholes (termed antidots) in a superconductor[12]. The vortex density can be varied continuously by applying an external magnetic field H and, as shown in Fig. 3a, their dynamics can be probed by measuring the voltage–current characteristics of the sample. Our sample is an Al film (with critical temperature $T_c = 1.437$ K) patterned by electron-beam lithography with a square array (with period $a_p = 1.5\,\mu$m) of neighbouring big and small antidots placed close to each other, thus generating an asymmetric double-well vortex trap with broken symmetry along the y direction only (Fig. 3b). As we have recently demonstrated, such a configuration provides efficient rectification of vortex motion at low fields[13,14].

Our experiment is carried out as follows: an oscillating driving force (generated by a sinusoidal transverse electrical current) is applied along the direction of broken symmetry, and the vortex motion in this direction is probed by measuring the transverse voltage (Fig. 3a). A phase diagram of vortex motion was obtained by detailed measurements of the root-mean-square and d.c. voltages (V_{rms} and V_{dc} respectively) across the sample (Fig. 3c). In the pinned vortex solid (PVS) phase, the applied current is not high enough to drive vortices out of their equilibrium positions. At some vortex densities (rational multiples of the first matching field, $H_1 = \Phi_0/a_p^2 = 0.92$ mT, where the number of vortices matches the number of double-traps), vortices assemble in a very stable lattice commensurate with the pinning array[15,16]. These special configurations enhance the critical current, producing the sharp re-entrances of the PVS phase at integer and half-integer matching fields. The moving vortex phase is dominated by ratchet dynamics exhibiting multiple drift reversals. From the first up to the fifth matching fields, the direction of net vortex motion changes its sign alternately, resembling the sign inversions of

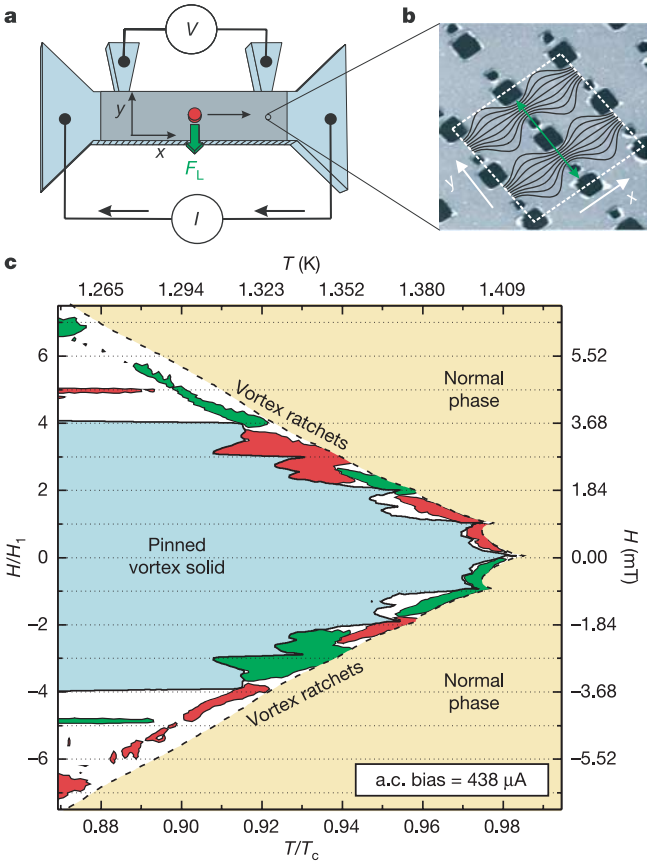

Figure 3 | Sample geometry and phase diagram of the vortex ratchet effect. a, The external magnetic field H generates a certain vortex distribution in the film. A vortex (shown schematically out of scale) is driven along the y direction by a Lorentz force $F_L = (J \times v)\Phi_0 d$ generated by an electrical current density J applied in the x direction (v is the normalized vortex circulation, parallel to H). If F_L is strong enough, vortices start moving along the drive with mean velocity v generating a voltage drop $V = L(v \times H)\cdot\hat{e}_x$ across a distance L. **b**, Atomic force micrograph of the double-antidot array (with period $a_p = 1.5\,\mu$m). The big and small antidots are 600×600 nm^2 and 300×300 nm^2 in size and separated by a 90-nm-thick superconducting wall. Details of the sample preparation and characteristics are given elsewhere[13]. The streamlines of the applied electrical current (shown schematically) are substantially denser between antidots than in the interstitial positions, forcing the vortices to move preferentially along the antidot rows. As the driving Lorentz force is always perpendicular to these lines, motion occurs along the broken symmetry (y) direction. **c**, H–T dynamical phase diagram at an a.c. current $I(t) = I_{ac}\sin(2\pi ft)$, with $I_{ac} = 438\,\mu$A ($J_{ac} = 3.95 \times 10^3$ A cm^{-2}) and $f = 1$ kHz. H_1 is the first matching field and T_c is the superconducting critical temperature. Between the pinned vortex solid and normal phases (compare Fig. 4), the voltage is dominated by vortex motion. The green and red areas correspond to positive and negative V_{dc} respectively. In the white areas, vortex motion is symmetric ($V_{dc} \approx 0$) within the experiment accuracy. Note that the rectification mechanism is insensitive to the vortex polarity, since the interaction of vortices or antivortices with a microhole is the same. This leads to a symmetric net d.c. velocity, $v_{dc}(H) = v_{dc}(-H)$, which then results in an antisymmetric d.c. voltage, $V_{dc}(H) = -V_{dc}(-H)$.

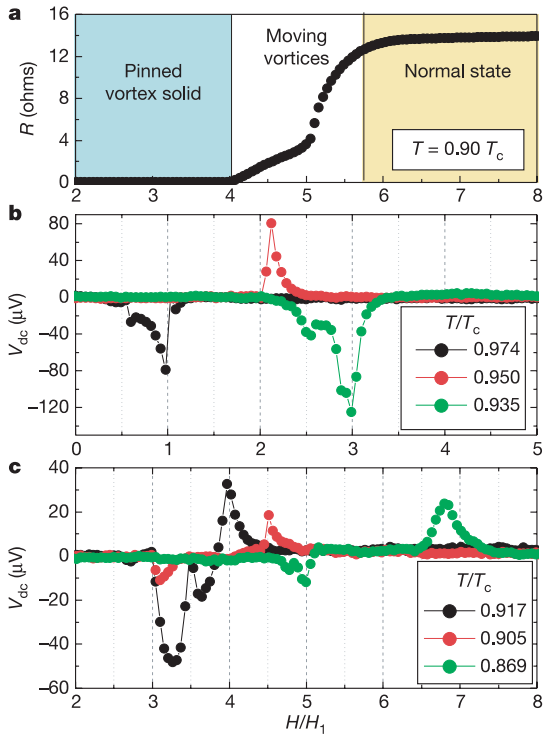

Figure 4 | Magnetoresistance and magnetic field dependence of the ratchet effect for an a.c. bias $I_{ac} = 438\,\mu$A. a, By performing a.c. magnetoresistance ($R(H) = \sqrt{2}V_{rms}/I_{ac}$) measurements, we determine the boundaries between the pinned vortex solid, moving vortices and normal phases. When vortices start moving, R increases towards the normal state resistance, R_n. The moving vortex phase is then bounded by the criteria $R = 10^{-5}R_n$, for the onset of vortex motion, and $R = 0.90R_n$, for the destruction of superconductivity. In **b** and **c**, the measured d.c. voltage, V_{dc}, is plotted against magnetic field for several temperature values. The curves exhibit multiple sign reversals of the d.c. voltage with maxima and minima close to integer and half-integer matching fields.

the chain drift in our 1D model (Fig. 2). Thermal fluctuations are negligible in our sample, because the pinning energy is typically much higher than kT ($U_p \approx 10^2 - 10^3\ kT$, for $T/T_c = 0.98 - 0.88$). Hence, the vortex dynamics is essentially deterministic. The temperature does however play an important role in determining the pinning efficiency of an antidot. At temperatures very close to T_c, vortices are bigger than the antidots, which then become less effective pinning centres. At lower temperatures, vortices become smaller and interact more strongly with the antidots[12]. In this sense, decreasing the temperature plays the role of increasing the pinning strength.

Sign reversal in a vortex ratchet has been reported previously for an array of triangular magnetic dots[17]. One single reversal was observed to take place gradually as the number of vortices increased above the corresponding saturation of the dots (three vortices per dot). This was interpreted as the effect of interstitial vortices moving in an inverted ratchet potential produced by the interactions with the trapped vortices. The multiple sign reversals observed in our experiment cannot be explained by the inverted ratchet effect of interstitial vortices. Rather, owing to the strong enhancement of the current density between the antidots (Fig. 3b), vortices tend to move in 1D channels along the antidot rows. These channels should however saturate at a high enough vortex concentration, the excess vortices being forced to move along the interstitial positions. It is also noteworthy that vortices are collective excitations; their cores can be deformed and merged into one another at extreme conditions. Consequently, one must be cautious when modelling vortices as hard particles. Nonetheless, the agreement of the experimental results with the model predictions is quite good, which suggests that the model is able to capture the main physics of the observed vortex ratchet effects. These multiple sign reversals provide a new tool for controlling and manipulating the motion of magnetic flux quanta in superconductors. Finally, we stress that our findings have a very general character and are also relevant to other ratchet systems of interacting particles, like charged colloidal suspensions in ratchet-like microtubules and ions in the selectivity filter of ion channels in cell membranes[4].

Received 17 June 2005; accepted 18 January 2006.

1. von Smoluchowski, M. Experimentell nachweisbare, der üblichen Thermodynamik widersprechende Molekularphänomene. *Phys. Z.* **13,** 1069–1080 (1912).
2. Feynman, R. P., Leighton, R. B. & Sands, M. *The Feynman Lectures On Physics* Ch. 46 Vol. 1 (Addison-Wesley, Reading, Massachusetts, 1966).
3. Magnasco, M. O. Forced thermal ratchets. *Phys. Rev. Lett.* **71,** 1477–1481 (1993).
4. Morais-Cabral, J. H., Zhou, Y. & MacKinnon, H. Energetic optimization of ion conduction rate by the K^+ selectivity filter. *Nature* **414,** 37–42 (2001).
5. Matthias, S. & Müller, F. Asymmetric pores in a silicon membrane acting as massively parallel brownian ratchets. *Nature* **424,** 53–57 (2003).
6. Bader, J. S. *et al.* DNA transport by a micromachined Brownian ratchet device. *Proc. Natl Acad. Sci. USA* **96,** 13165–13169 (1999).
7. Bartussek, R., Hänggi, P. & Kissner, J. G. Periodically rocked thermal ratchets. *Europhys. Lett.* **28,** 459–464 (1994).
8. Derényi, I. & Vicksec, T. Cooperative transport of Brownian particles. *Phys. Rev. Lett.* **75,** 374–377 (1995).
9. Savel'ev, S., Marchesoni, F. & Nori, F. Controlling transport in mixtures of interacting particles using Brownian motors. *Phys. Rev. Lett.* **91,** 010601 (2003).
10. Mateos, J. L. Chaotic transport and current reversal in deterministic ratchets. *Phys. Rev. Lett.* **84,** 258–261 (2000).
11. Risken, H. *The Fokker-Planck Equation* Ch. 11 (Springer, New York, 1984).
12. Blatter, G., Feigel'man, M. V., Geshkenbein, V. B., Larkin, A. I. & Vinokur, V. M. Vortices in high-temperature superconductors. *Rev. Mod. Phys.* **66,** 1125–1388 (1994).
13. de Souza Silva, C. C., Van de Vondel, J., Zhu, B. Y., Morelle, M. & Moshchalkov, V. V. Vortex ratchet effects in films with a periodic array of antidots. *Phys. Rev. B* **73,** 014507 (2006).
14. Van de Vondel, J., de Souza Silva, C. C., Zhu, B. Y., Morelle, M. & Moshchalkov, V. V. Vortex-rectification effects in films with periodic asymmetric pinning. *Phys. Rev. Lett.* **94,** 057003 (2005).
15. Fiory, A. T., Hebard, A. F. & Somekh, S. Critical currents associated with the interaction of commensurate flux-line sublattices in a perforated Al film. *Appl. Phys. Lett.* **32,** 73–75 (1977).
16. Baert, M., Metlushko, V. V., Jonckheere, R., Moshchalkov, V. V. & Bruynseraede, Y. Composite flux-line lattices stabilized in superconducting films by a regular array of artificial defects. *Phys. Rev. Lett.* **74,** 3269–3272 (1995).
17. Villegas, J. E. *et al.* A superconducting reversible rectifier that controls the motion of magnetic flux quanta. *Science* **302,** 1188–1191 (2003).

Supplementary Information is linked to the online version of the paper at www.nature.com/nature.

Acknowledgements We thank A. Silhanek for the critical reading of our paper and S. Raedts for taking the AFM micrographs. This work was supported by the K.U. Leuven Research Fund GOA and FWO programmes. C.C.d.S.S. was supported by CNPq, an Agency of the Brazilian Government.

Author Information Reprints and permissions information is available at npg.nature.com/reprintsandpermissions. The authors declare no competing financial interests. Correspondence and requests for materials should be addressed to V.V.M. (Victor.Moshchalkov@fys.kuleuven.be).